Numerical Modeling and Uncertainty Analysis of Downhole Low-Frequency Electromagnetic Transmission

Dongxiao Pang[1*], Huiyan Hou[2], Jinjun Bai[2], and Xiong Han[1]

[1]Drilling and Production Engineering Technology Research Institute
CNPC Chuanqing Drilling Engineering Co. Ltd., Guanghan, Sichuan 618300, China
dongxx_zyy@cnpc.com.cn, hanx_ccde@cnpc.com.cn

[2]Department of Electrical Engineering
Dalian Maritime University, Dalian 116026, China
hhy1120241357@dlmu.edu.cn, baijinjun@dlmu.edu.cn
*Corresponding author

Abstract – As oil and gas resource development extends into increasingly complex geological conditions, reliable downhole signal transmission has become a critical challenge in drilling and measurement-while-drilling (MWD) operations. In engineering practice, downhole low-frequency electromagnetic wave (LF-EM) transmission is widely used as an important means of downhole data telemetry because of its low dependence on drilling fluid. However, uncertainties in formation properties and fluctuations in geological parameters can significantly affect electromagnetic signal transmission, making it difficult for surface systems to stably receive downhole information in practical applications. To address this issue, a transmission channel model for downhole LF-EM is established based on FEKO. First, sensitivity analysis is performed to identify the key uncertainty parameters that have the most significant influence on signal attenuation. Then, the Kriging method and the Stochastic Collocation Method (SCM) are employed to conduct uncertainty analysis and to obtain the probability density function (PDF) of the received magnetic-field strength within the parameter fluctuation range. To compare the reliability and applicability of the two methods, Monte Carlo Method (MCM) simulation is adopted as the benchmark, and the Mean Equivalent Area Method (MEAM) is introduced for comprehensive evaluation. Results show that the SCM exhibits overall better fitting accuracy and computational stability than the Kriging method, making it more suitable for probabilistic prediction and risk assessment of downhole low-frequency electromagnetic transmission.

Index Terms – Downhole signal transmission, low-frequency electromagnetic waves, sensitivity analysis, uncertainty analysis.

I. INTRODUCTION

As oil and gas exploration and development continue to advance toward deep, ultra-deep, and more complex geological environments, the stable and efficient transmission of downhole signals has become a critical challenge in drilling and measurement-while-drilling (MWD) operations [1, 2]. Among various downhole wireless telemetry technologies, low-frequency electromagnetic wave communication, owing to its strong medium penetration capability and relatively long effective transmission distance, can overcome the limitations of conventional communication methods to a certain extent and provide important support for real-time data transmission and downhole condition monitoring [3, 4]. However, the diversity of formation media, together with the spatial heterogeneity of electromagnetic parameters such as electrical conductivity and permittivity, can lead to significant energy attenuation of low-frequency electromagnetic wave signals and even cause communication interruption [5–7], thereby reducing the reliability of this technology under complex formation conditions and limiting its engineering applicability. Therefore, this study focuses on the simulation and prediction of low-frequency electromagnetic wave propagation under geological multi-parameter uncertainty. By characterizing and predicting the statistical behavior of the received signals, the proposed framework provides quantitative support for engineering design and risk assessment.

To characterize the propagation process of downhole low-frequency electromagnetic wave (LF-EM), numerical electromagnetic simulation generally adopts mainstream numerical methods such as the finite-difference time-domain method (FDTD), the finite element method (FEM), and the Method of Moments (MoM), along with various improved and hybrid

Submitted On: April 01, 2026
Accepted On: July 24, 2026

1054-4887 © ACES

https://doi.org/10.13052/2026.ACES.J.410709

strategies derived from them [8]. For the downhole low-frequency propagation scenario considered in this paper, the electrical size of the model is relatively small, and the MoM provides a good balance between computational accuracy and efficiency. Previous studies have shown that Streich and Swidinsky established an electromagnetic source model with metallic wellbore coupling based on the MoM and analyzed the spatial distribution characteristics of electromagnetic fields in layered formations [9]. Wang et al. developed a propagation model for extremely low-frequency electromagnetic waves in wellbores and stratified formations, and verified its effectiveness through both simulations and experiments [10]. In recent years, [11] proposed a numerical model based on the two-dimensional MoM for low-frequency electromagnetic problems, systematically analyzing the effects of different discretization schemes on computational accuracy and numerical stability, thereby providing theoretical support for efficient simulation. Based on the above considerations, this paper adopts the MoM and performs the solution using the three-dimensional full-wave electromagnetic simulation platform FEKO. Its low-frequency stabilization technique can effectively alleviate the numerical instability of the conventional MoM at extremely low frequencies, thereby saving computational resources while maintaining computational accuracy.

Under this simulation framework, non-intrusive uncertainty quantification methods are adopted in this study to address the uncertainty of formation parameters, including Stochastic Reduced Order Models (SROM) [12], MoM [13], Monte Carlo Method (MCM) [14, 15], Kriging method [16], and Stochastic Collocation Method (SCM) [17]. Among these methods, both SROM and the MoM are computationally efficient, but their accuracy is usually limited. The MCM is widely regarded as a reliable benchmark, but its computational cost becomes significant when the cost of a single simulation is high. In contrast, the Kriging method and SCM offer better overall trade-offs between efficiency and accuracy, although they still face the problem of large computational scale in high-dimensional parameter spaces. In addition, the computational cost of a single FEKO simulation grows with the dimensionality of the random parameter space. To alleviate this issue, the sensitivity-analysis-based random variable reduction strategy proposed in [18] can be used to screen key random variables during the preprocessing stage, thereby effectively improving the computational efficiency of uncertainty analysis methods.

Based on the above methodology, this study investigates the uncertainty arising from random variations in formation conductivity and layer thickness within a FEKO-based low-frequency electromagnetic transmission model. First, sensitivity analysis is employed to identify the dominant uncertainty parameters and reduce the dimensionality of the random variable space. Subsequently, Kriging and SCM surrogate models are developed to characterize and predict the statistical response of the received magnetic field intensity under parameter uncertainty. MCM is adopted as a benchmark for evaluating the two approaches in terms of computational efficiency, probability density function (PDF) fitting performance, and errors in key statistical measures. Furthermore, to quantitatively assess the prediction accuracy, Mean Equivalent Area Method (MEAM) proposed in [19] is introduced. Combined with statistical indicators, including the mean, variance, relative error, and computational cost, a comprehensive evaluation of the predictive performance of different methods is conducted. The proposed framework provides an effective approach for uncertainty quantification of low-frequency electromagnetic wave propagation in downhole communication channels and offers quantitative support for engineering design and risk assessment.

The structure of this paper is as follows. Section II introduces the modeling process of the low-frequency electromagnetic transmission channel based on FEKO. Section III presents parameter preprocessing using sensitivity analysis. Section IV describes the procedures of uncertainty analysis based on the Kriging method and SCM, and comparatively evaluates the two methods. Section V concludes the paper.

II. LF-EM TRANSMISSION CHANNEL MODELING USING FEKO

In the downhole wireless direct-reading system (Fig. 1), the transmitting tool is lowered along the tubing to the target formation, where downhole production or environmental data are acquired and then transmitted

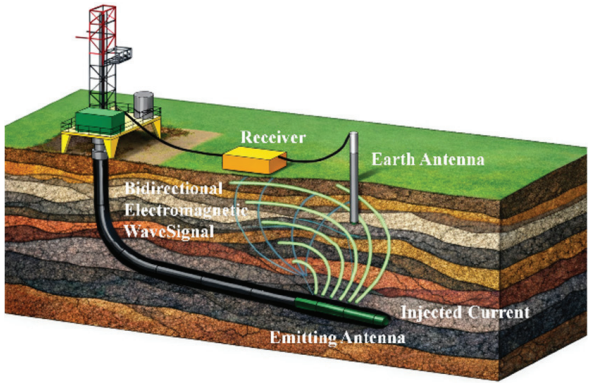


Fig. 1. Electromagnetic-wave-based downhole wireless direct-reading system.

to the surface through low-frequency electromagnetic waves. The surface receiver performs signal reception, demodulation, and decoding, thereby establishing a downhole-to-surface wireless transmission link [20]. However, due to the intricacy of the formation system, signal transmission may fail under complex formation conditions. The spatially non-uniform distribution of salinity, mineralization, and medium composition in the formation results in significant spatial variability and uncertainty in electromagnetic parameters, such as electrical conductivity and relative permittivity, at different depths. In addition, formation interfaces often appear as transition zones rather than clear boundaries, which leads to uncertainty in layer division and parameter assignment. Moreover, when constructing a continuous FEKO formation model from discrete data, assumptions are inevitably introduced. Therefore, statistically derived geometric parameters, such as formation thickness, are more appropriately characterized by interval estimation.

To achieve a balance between computational tractability and geological realism, this study is based on the measured formation data from the Yishan Slope of the Ordos Basin, and the formation layers are statistically grouped according to the ranges of electrical conductivity. For layers with stable lithology, small dispersion, and relatively weak influence on signal transmission, deterministic parameters are constructed using the weighted average method. For layers with strong heterogeneity, significant fluctuations, and dominant influence on transmission, the parameter intervals are retained to characterize their uncertainty.

As a result, the complex formation is equivalently represented by a nine-layer stratified FEKO medium model, and the electrical conductivity and layer thickness of each layer are listed in Table 1. The core of the transmitter is a loop antenna operating under a given working frequency and excitation current. To reduce the complexity of FEKO modeling, it is equivalently represented in this paper by a magnetic dipole source in the form of a current loop with a known time-varying current. The time-varying electromagnetic field excited by the magnetic dipole source induces eddy currents in the formation, which further radiate secondary magnetic fields. In this way, signal transmission along the wellbore direction is achieved through a continuous "magnetic-to-electric-to-magnetic" induction process. Finally, the received magnetic-field strength on the top plane of the FEKO model is taken as the signal reception value. The simulation flow for electromagnetic transmission channel modeling from the deepest downhole position to the wellhead is shown in Fig. 2.

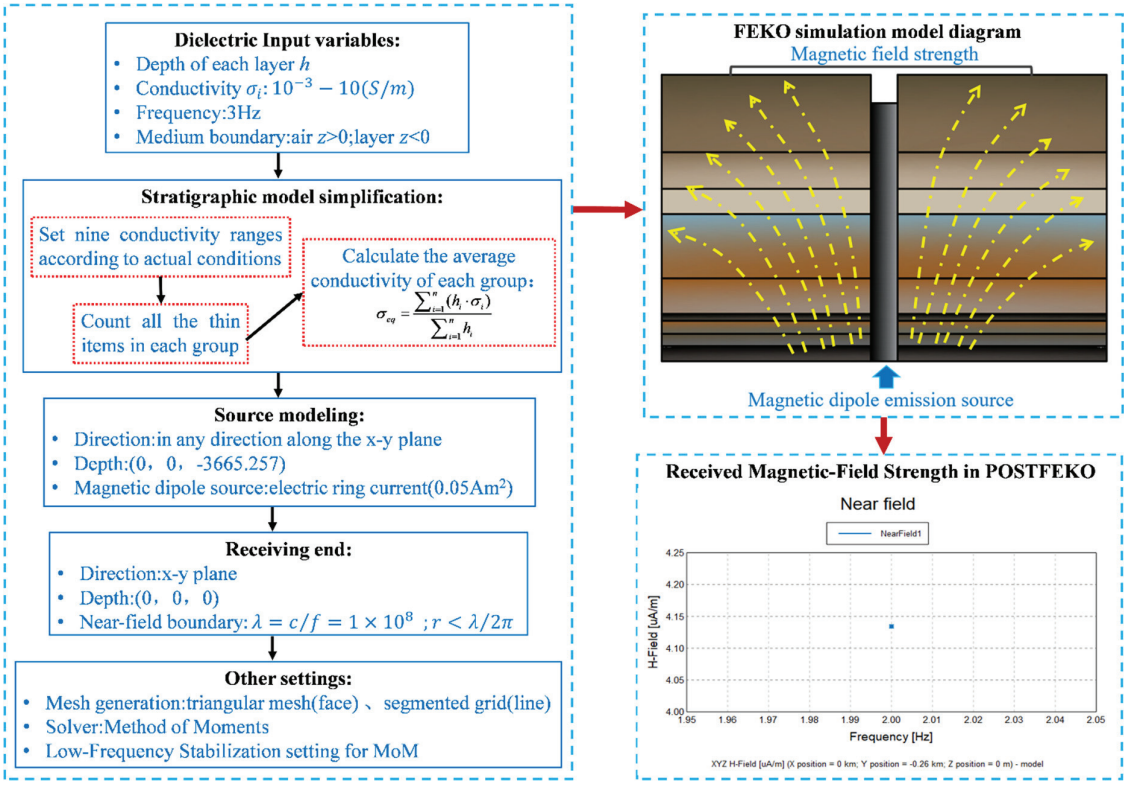


Fig. 2. FEKO-based simulation flowchart.

Table 1: Parameters of the nine-layer geological model in FEKO

Formation Group	**1**	**2**	**3**	**4**
Electrical Conductivity (S/m)	[5.5, 6.2]	[0.32, 0.8]	0.0865	[1, 2.1]
Layer Thickness (m)	[1017.5, 1296.5]	329.5	229	[1330, 1382]
5	**6**	**7**	**8**	**9**
0.015	0.0072	0.00385	[0.0007, 0.001]	0.00003
320.75	[47.25, 175.5]	23.5	112.5	50

$$
\begin{aligned}
IS_{pos}(i) = \frac{dy_\xi}{d\xi_i} &= 2 \times \frac{U_{FEKO}\left(\bar{\xi}_1, \ldots, \bar{\xi}_i + \frac{\delta_i}{2}, \ldots, \bar{\xi}_n\right) - U_{FEKO}\left(\bar{\xi}_1, \ldots, \bar{\xi}_i, \ldots, \bar{\xi}_n\right)}{\frac{\delta_i}{2}} \\
&- \frac{U_{FEKO}\left(\bar{\xi}_1, \ldots, \bar{\xi}_i + \delta_i, \ldots, \bar{\xi}_n\right) - U_{FEKO}\left(\bar{\xi}_1, \ldots, \bar{\xi}_i, \ldots, \bar{\xi}_n\right)}{\delta_i} + o(\delta_i) \\
IS_{neg}(i) = \frac{dy_\xi}{d\xi_i} &= 2 \times \frac{U_{FEKO}\left(\bar{\xi}_1, \ldots, \bar{\xi}_i - \frac{\delta_i}{2}, \ldots, \bar{\xi}_n\right) - U_{FEKO}\left(\bar{\xi}_1, \ldots, \bar{\xi}_i, \ldots, \bar{\xi}_n\right)}{\frac{\delta_i}{2}} \\
&- \frac{U_{FEKO}\left(\bar{\xi}_1, \ldots, \bar{\xi}_i - \delta_i, \ldots, \bar{\xi}_n\right) - U_{FEKO}\left(\bar{\xi}_1, \ldots, \bar{\xi}_i, \ldots, \bar{\xi}_n\right)}{\delta_i} + o(\delta_i).
\end{aligned} \tag{1}
$$

III. SENSITIVITY ANALYSIS AND RANDOM-VARIABLE REDUCTION

During the transmission of downhole LF-EM, uncertainties in formation, medium parameters can significantly affect signal propagation characteristics. Uncertainty analysis aims to characterize the response behavior of simulation outputs under perturbations in random input parameters. Since different input variables contribute unequally to the output response, the fast sensitivity analysis approach proposed in [18] is adopted to identify the relative importance of uncertain input variables. This method is based on a one-at-a-time (OAT) perturbation strategy, in which only a single input parameter is varied while all remaining parameters are maintained at their nominal values, thereby avoiding the high-dimensional combinatorial computations associated with simultaneous perturbations of all variables. Compared with direct uncertainty propagation involving the entire random parameter space, the OAT approach typically requires only local updates of model parameters, resulting in reduced geometric modifications, mesh reconstruction efforts, and computational costs. Consequently, sensitivity indices of the input parameters can be efficiently obtained at a relatively low computational expense. Subsequently, random variables with negligible sensitivity are replaced by their mean values, thereby achieving random variable reduction and reducing the dimensionality of the uncertainty space. The calculation procedure is described as shown in (1). After obtaining the sensitivity evaluation results under positive perturbation $IS_{pos}(i)$ and negative perturbation $IS_{neg}(i)$, the method constructs a comprehensive sensitivity index $IS(i)$ by averaging and combining the results from both sides:

$$IS(i) = |IS_{pos}(i)| + |IS_{neg}(i)|. \tag{2}$$

The relative contribution of each random variable to the output response can be obtained through normalization:

$$P(i) = \frac{IS(i)}{\sum_{i=1}^{N} IS(i)}, \tag{3}$$

where $\bar{\xi}_i$ is the mean of random variable ξ_i, and $U_{EFKO}(\bar{\xi}_1, \ldots, \bar{\xi}_i, \ldots, \bar{\xi}_n)$ is the received magnetic-field strength obtained from the FEKO simulation at the deterministic point $\{\bar{\xi}_1, \ldots, \bar{\xi}_i, \ldots, \bar{\xi}_n\}$. For the uncertainty parameter $k(\xi_i) = A + B \times \xi_i$, ξ_i denotes a uniformly distributed random variable over $[-1, 1]$, the mean and variance of the uncertain input parameter are k_M and k_σ, respectively, where $\begin{cases} k_M = A \\ k_\sigma = \frac{1}{3}B^2 \end{cases}$. Here, $\delta_i = \frac{\sqrt{3k_\sigma}}{k_M}$ is a small perturbation quantity. $S(i)$ denotes the sensitivity analysis result associated with random variable ξ_i, and $o(\delta_i)$ denotes the approximation error.

Based on the FEKO simulation model for downhole LF-EM transmission, seven groups of uncertain inputs exhibiting significant fluctuations in the measured data are selected in this study, as defined in (4), for sensitivity analysis. These include the electrical conductivity of the first layer $\sigma_1(\xi)$, second layer $\sigma_2(\xi)$, fourth layer $\sigma_4(\xi)$, and eighth layer $\sigma_8(\xi)$, as well as the thickness of the first layer $h_1(\xi)$, fourth layer $h_4(\xi)$, and

Table 2: Sensitivity analysis results for the seven groups of fluctuating parameters

Uncertainty Parameters	$\sigma_1(\xi)$	$\sigma_2(\xi)$	$\sigma_4(\xi)$	$\sigma_8(\xi)$	$h_1(\xi)$	$h_4(\xi)$	$h_6(\xi)$
Sensitivity Index	1.94%	1.81%	52.28%	0.07%	42.04%	1.26%	0.6%

sixth layer $h_6(\xi)$. The received magnetic-field strength obtained through POSTFEKO post-processing is then systematically evaluated.

$$\begin{aligned}
\sigma_1(\xi_1) &= 5.85 + 0.35 \times \xi_1 \text{ [s/m]} \\
\sigma_2(\xi_2) &= 0.56 + 0.24 \times \xi_2 \text{ [s/m]} \\
\sigma_4(\xi_3) &= 1.55 + 0.55 \times \xi_3 \text{ [s/m]} \\
\sigma_8(\xi_4) &= 0.00085 + 0.00015 \times \xi_4 \text{ [s/m]} \\
h_1(\xi_5) &= 1157 + 139.5 \times \xi_5 \text{ [m]} \\
h_4(\xi_6) &= 1356 + 26 \times \xi_6 \text{ [m]} \\
h_6(\xi_7) &= 111.375 + 64.125 \times \xi_7 \text{ [m]}
\end{aligned} \tag{4}$$

where $\xi_1, \xi_2, \xi_3, \xi_4, \xi_5, \xi_6$ and ξ_7 are uniformly distributed random variables over the interval $[-1, 1]$.

The sensitivity analysis results are presented in Table 2. The parameters $\sigma_1(\xi), \sigma_2(\xi), \sigma_8(\xi), h_4(\xi)$, and $h_6(\xi)$ account for less than 2% of the total weight, indicating that their effects on the output are negligible. Therefore, in the subsequent uncertainty analysis, they are equivalently replaced by their mean values according to (5).

$$\begin{aligned}
\sigma_1(\xi_1) &= 5.85 \\
\sigma_2(\xi_2) &= 0.56 \\
\sigma_8(\xi_4) &= 0.00085 \\
h_4(\xi_6) &= 1356 \\
h_6(\xi_7) &= 111.375.
\end{aligned} \tag{5}$$

In summary, the sensitivity analysis achieves random variable reduction during the preprocessing stage, accurately quantifies the influence of each formation parameter on the received magnetic-field strength obtained in POSTFEKO, and identifies the electrical conductivity of the fourth layer $\sigma_4(\xi)$ and the thickness of the first layer $h_1(\xi)$ as the dominant factors affecting electromagnetic wave signal attenuation. This provides clear guidance for surrogate model construction in the subsequent uncertainty analysis.

IV. UNCERTAINTY ANALYSIS USING KRIGING AND SCM

A. Kriging

The Kriging method is a surrogate modeling approach based on statistical learning. Its central idea is to generate multiple sets of deterministic parameters using Latin Hypercube Sampling (LHS), obtain the corresponding deterministic simulation results through numerical simulations, and then use these results to train and construct a surrogate model. The surrogate model is subsequently used as an approximate substitute for the complex original model in uncertainty analysis. The basic procedure is illustrated in Fig. 3. In this study, the high-sensitivity parameters identified by sensitivity analysis are selected as uncertain inputs. A twodimensional parameter space is constructed using the electrical conductivity of the fourth layer over the interval [1, 2.1] S/m and the thickness of the first layer over the interval [1017.5, 1296.5] m. LHS is then employed to generate nine training samples so as to cover representative regions of the parameter space, and the resulting sampling point vectors are given as shown in (6). A deterministic FEKO simulation in (7) is performed for each sample to obtain the corresponding received magnetic-field strength:

$$\begin{aligned}
S_{\text{Kriging}}(K) &= [X_1, X_2] \\
X_1 &= [1.47, 1.48, 1.854, 1.589, 2.049, 1.599, \\
&\quad 1.09, 1.403, 1.936]^T (s/m) \\
X_2 &= [1064.71, 1099.25, 1163.72, 1117, \\
&\quad 1030.24, 1291.8, 1140.64, 1158.12, \\
&\quad 1107.77]^T (m)
\end{aligned} \tag{6}$$

$$\begin{aligned}
Y_{FEKO} &= [9.08, 6.94, 2.688, 5.287, 5.73, 1.432, \\
&\quad 8.7, 4.97, 3.686] (mA/m),
\end{aligned} \tag{7}$$

where K denotes the sample index generated by Latin Hypercube Sampling. The training input matrix is $S \in \mathbb{R}^{9\times 2}$, and the corresponding output vector is $Y \in \mathbb{R}^9$. Each row of S corresponds to one LHS sample, and the associated entry of Y denotes the received magnetic-field strength obtained from the FEKO simulation.

The training set $\{S_{Kriging}(K), Y_{FEKO}\}$ for surrogate model construction is thus obtained. By selecting an appropriate fitting model, a surrogate model can be established to approximately represent the response surface of the FEKO model within the parameter space. Based on the trained surrogate model, a large number of prediction samples can be rapidly generated within the parameter fluctuation range (1600 samples in this

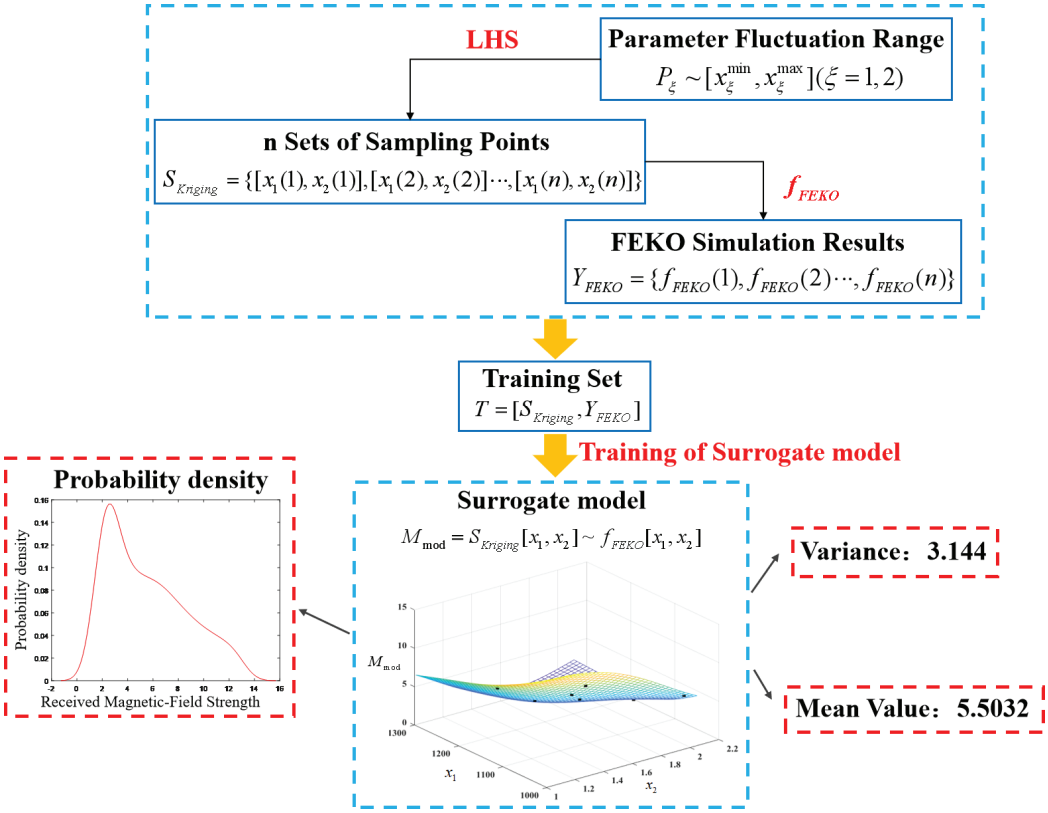


Fig. 3. Schematic illustration of the Kriging method (two-dimensional example).

study), from which the PDF of the received magnetic-field strength can be estimated. In this way, efficient statistical analysis and rapid prediction of the output distribution can be achieved.

B. SCM

SCM is an efficient uncertainty quantification approach based on Polynomial Chaos Expansion (PCE). Its central idea is to represent the output of a stochastic system as a polynomial function of the input random variables by means of orthogonal polynomial expansion. The specific procedure is illustrated in Fig. 4. For the two-dimensional uncertainty case, the random vector is defined as $X = \{X_1, X_2\}$. According to the generalized polynomial chaos theory, the zeros $\{z_1, \ldots, z_n\}$ of the chaos polynomial are then selected and combined in tensor-product form to generate the collocation points [17]. Let $X_1 = \{x_1^1, x_1^2, \ldots, x_1^9\}$ and $X_2 = \{x_2^1, x_2^2, \ldots, x_2^9\}$ denote the one-dimensional collocation nodes associated with the two uncertain variables. The two-dimensional collocation set is then constructed by their tensor product. Therefore, a total of $9 \times 9 = 81$ collocation points are obtained, as shown in (8).

By conducting multiple deterministic FEKO simulations at the collocation points $p(X)$ and then applying multidimensional Lagrange interpolation, the polynomial response with respect to the random variables can be obtained as shown in (8).

$$\begin{aligned} X_1 &= [1.124, 1.124, 1.124, 1.976, 1.976, 1.976, \\ &\quad 1.55, 1.55, 1.55](\text{s/m}) \\ X_2 &= [1048.9, 1261.5, 1157, 1048.9, 1261.5, \\ &\quad 1157, 1048.9, 1261.5, 1157](\text{m}), \\ p(X) &= X_1 \otimes X_2 = \{(x_1^i, x_2^j) \mid i, j = 1, \ldots, 9\} \end{aligned} \tag{8}$$

$$M_{FEKO}(X) = \sum_{i=0}^{n^2} \text{FEKO}[p_i(X)] L_i[p_i(X), p(X), X] \tag{9}$$

where $FEKO[p_i(X)]$ denotes the deterministic simulation result at collocation point $p_i(X)$, and $L_i[p_i(X), p(X), X]$ denotes the value of the multidimensional Lagrange interpolation polynomial evaluated at $p_i(X)$. Here, $M_{FEKO}(X)$ can be regarded as the trained surrogate model. By further substituting 5000 randomly sampled points within the fluctuation range into $M_{FEKO}(X)$, the uncertainty analysis results of the received magnetic-field strength can be efficiently obtained.

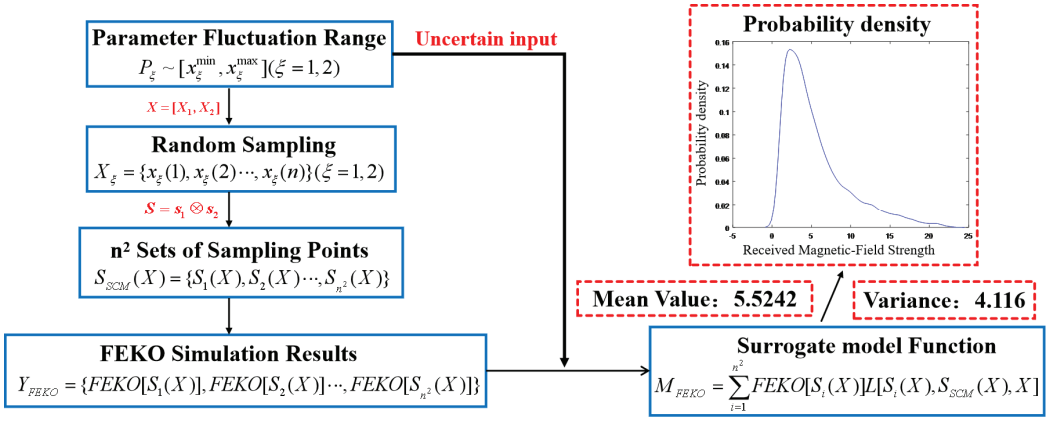


Fig. 4. Schematic illustration of the SCM (two-dimensional example).

C. Accuracy validation

Both surrogate models employed for uncertainty analysis were trained using the same set of nine sampling points. After model construction, 1600 prediction samples and 5000 prediction samples were generated for the Kriging and SCM models, respectively, to estimate PDF of the received magnetic field intensity. It should be noted that the difference in the number of prediction samples only affects the smoothness of the resulting PDF curves and does not influence the predictive accuracy of the surrogate models.

To evaluate the accuracy of the uncertainty analysis results obtained using the Kriging and SCM approaches, an additional set of 500 test samples was generated within the variation ranges of the high-sensitivity parameters using LHS. Corresponding outputs were obtained through FEKO simulations for each sample. Taking the PDF generated by MCM as the reference benchmark, the statistical predictions of the two surrogate-based approaches were compared and validated. The results indicate that the PDF curves predicted by both Kriging and SCM exhibit good agreement with the MCM benchmark within the principal probability region and capture the overall trend of the output distribution. This suggests that both surrogate models are capable of reproducing the uncertainty characteristics of the received magnetic field intensity. To further assess the reliability of the two uncertainty analysis approaches, PDF comparisons obtained using nine and 36 training samples are presented in Fig. 5. When only nine training samples are employed, the SCM prediction shows closer agreement with the MCM benchmark in terms of distribution width and the right-tail region, whereas the Kriging model still exhibits noticeable deviations. When the number of training samples is increased to 36, the PDFs predicted by both surrogate models become nearly indistinguishable from the MCM result. These observations indicate that SCM can achieve satisfactory prediction accuracy with relatively few training samples, whereas the performance of Kriging is more sensitive to the sample size.

Furthermore, quantitative comparisons of the mean, variance, and their relative errors (Table 3) reveal that the statistical measures predicted by SCM are consistently closer to the MCM benchmark and exhibit greater stability with increasing sample size. In contrast, Kriging shows larger errors under small-sample conditions and a relatively weaker capability to capture the complete characteristics of the probability distribution. Overall, under the conditions considered in this study, SCM demonstrates superior accuracy, robustness, and distribution-reconstruction capability compared with Kriging, particularly in the small-sample regime.

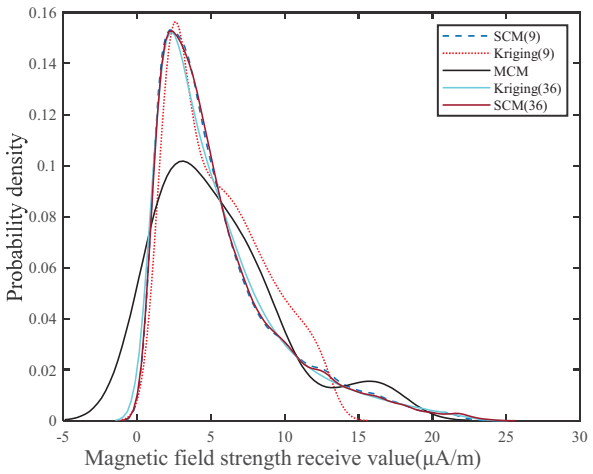


Fig. 5. Comparison of probability density functions.

To quantitatively assess the computational efficiency of the two uncertainty analysis methods, convergence studies were performed by progressively

Table 3: Comparison of statistical metrics

Statistical Metric	Mean Value	Variance	Relative Error of Mean Value	Relative Error of Variance
MCM	5.5326	4.1888	0	0
Kriging (9)	5.5032	3.1440	00.53%	24.94%
SCM (9)	5.5242	4.1160	00.15%	1.74%
Kriging (36)	5.4704	4.1390	1.12%	1.19%
SCM (36)	5.5254	4.1432	0.13%	1.09%

Table 4: Similarity to MCM versus number of training samples

Number of Sample Sets	9	16	25	36
Kriging-MCM Similarity	75.1%	84.56%	89.44%	92.96%
SCM-MCM Similarity	98.2%	98.65%	98.94%	99.05%

Table 5: Comparison of computational time

Analysis Method	Sensitivity Analysis Time (min)	Number of Model Evaluations	Total FEKO Simulation Time (min)	Algorithm Execution Time (min)	Total Computational Time (min)	Sensitivity Analysis Time Ratio
MCM	14.5	5000	2500	0.1	2514.6	0.58%
SCM	14.5	9	4.5	0.5	19.5	74.36%
Kriging	14.5	36	18	3.2	35.7	40.62%

increasing the number of training samples. MEAM was adopted to quantify the similarity between the predicted and reference distributions. Owing to the tensor-product construction of SCM, the number of collocation points in the two-dimensional parameter space is limited to perfect squares. Consequently, experiments were conducted using 9, 16, 25, and 36 training samples, and the corresponding similarity values are summarized in Table 4. Based on these results, the computational cost required to achieve a similarity level of 90% was further evaluated and compared.

As shown in Table 4, when only nine training samples were employed, the similarity between the SCM prediction and the MCM benchmark reached 98.2%, which was substantially higher than the 75.1% achieved by the Kriging model. When the number of training samples was increased to 36, the similarity between the Kriging prediction and the MCM benchmark also exceeded 90%, indicating that both surrogate models can achieve satisfactory prediction accuracy with sufficient training samples. The computational time of a single FEKO simulation was approximately 0.5 min. A total of $4 \times 7 + 1 = 29$ FEKO simulations were required for the sensitivity analysis procedure, corresponding to a computational cost of approximately 14.5 min. The total computational times of the different methods are summarized in Table 5. It can be observed that the computational cost of MCM is significantly higher than those of the surrogate-based uncertainty analysis approaches. Furthermore, SCM achieves higher similarity to the benchmark solution while requiring less computational effort than Kriging.

These results indicate that SCM provides a more favorable balance between prediction accuracy and computational cost. Therefore, for the low-frequency electromagnetic transmission uncertainty problem considered in this study, SCM exhibits superior predictive performance, computational efficiency, and numerical robustness.

V. CONCLUSION

This paper investigates the uncertainty of formation parameters in the low-frequency electromagnetic wave transmission system for downhole wireless direct-reading technology. Based on measured formation data, a refined nine-layer stratified geological model is established, and the downhole-to-surface transmission channel is modeled and solved using the FEKO electromagnetic simulation platform. First, preprocessing based on sensitivity analysis indicates that the electrical conductivity of the fourth layer and the thickness of the first layer are the key fluctuating parameters affecting electromagnetic wave signal attenuation. Subsequently, the Kriging method and the SCM are employed to obtain the PDF of the received magnetic-field strength under fluctuations of the high-sensitivity parameters. Compared with the MCM, the PDFs obtained by the two methods exhibit a high degree of agreement with

the MCM in terms of both the overall trend and the high-probability-density region, thereby verifying their statistical accuracy in uncertainty analysis. Finally, the MEAM is introduced to quantitatively evaluate the similarity between the predicted distributions and the reference distribution. The results demonstrate that SCM outperforms Kriging in terms of both distribution-fitting quality and computational efficiency. Furthermore, the predicted statistical measures, including the mean and variance, are in closer agreement with the benchmark solution. These findings indicate that SCM provides higher predictive accuracy and greater numerical robustness for the low-frequency electromagnetic transmission uncertainty problem investigated in this work.

ACKNOWLEDGEMENT

This paper is supported by the General Project of Liaoning Province, No. 2025-MS-092.

REFERENCES

[1] J. Sun, J. Yang, Y. Bai, K. Lyu, and F. Liu, "Research progress and development of deep and ultra-deep drilling fluid technology," *Petroleum Exploration and Development*, vol. 51, no. 4, pp. 1022–1034, 2024.

[2] A. E. Ibhaze, D. O. Akinola, A. L. Imoize, P. E. Orukpe, and F. O. Edeko, "A review of downhole communication technologies," *Journal of Telecommunication, Electronic and Computer Engineering*, vol. 14, no. 4, pp. 1–10, 2022.

[3] Y. Wu, F. Wang, J. Li, B. Wang, and D. Pang, "Wireless electromagnetic telemetry for metal cased wells: A novel approach with comprehensive channel analysis," *Geoenergy Science and Engineering*, vol. 233, no. 212573, 2024.

[4] Z. Li, J. Lin, S. Xing, X. Ji, M. Dang, and J. Wang, "A novel wireless electromagnetic wave transmission method applicable to water injection wells and analysis of the influence factors," *Scientific Reports*, vol. 15, no. 17230, 2025.

[5] C. Shao, L. Xu, X. Chen, Z. Chu, and B. Yang, "Factors affecting received signal intensity of electromagnetic measurement-while-drilling during underground in-seam horizontal drilling," *Journal of Natural Gas Science and Engineering*, vol. 56, pp. 212–221, 2018.

[6] Z. Wang, D. Jia, F. Sun, Z. Hao, and Q. Chen, "Network model and application in wellbore wireless communication of extremely low-frequency electromagnetic waves," *Journal of Geophysics and Engineering*, vol. 22, no. 3, pp. 672–681, 2025.

[7] H. Li, X. Chen, Y. Meng, Y. Chen, G. Li, and C. Xu, "A novel method for wireless telemetry during air drilling based on air pressure pulses," *Geoenergy Science and Engineering*, vol. 234, no. 212669, 2024.

[8] P. Sumithra and D. Thiripurasundari, "A review on computational electromagnetics methods," *Advanced Electromagnetics*, vol. 6, no. 1, pp. 42–55, 2017.

[9] R. Streich and A. Swidinsky, "On method-of-moments modelling of electromagnetic sources connected to metallic well casings," *Geophysical Journal International*, vol. 234, no. 2, pp. 1476–1483, 2023.

[10] Z. Wang, D. Jia, F. Sun, Q. Chen, S. Zhu, and Q. Wang, "Research on extremely low frequency electromagnetic wave model and simulation in wellbore communication," *Scientific Reports*, vol. 14, no. 20093, 2024.

[11] J. A. Luta, C. A. Castillo, D. C. Horvath, R. A. Howard, and S. D. Pekarek, "2-D method of moments formulations for nonlinear low-frequency electromagnetics," *Engineering Analysis with Boundary Elements*, vol. 179, no. 106383, 2025.

[12] Z. Fei, Y. Huang, J. Zhou, and Q. Xu, "Uncertainty quantification of crosstalk using stochastic reduced order models," *IEEE Transactions on Electromagnetic Compatibility*, vol. 59, no. 1, pp. 228–239, 2016.

[13] R. S. Edwards, A. C. Marvin, and S. J. Porter, "Uncertainty analyses in the finite-difference time-domain method," *IEEE Transactions on Electromagnetic Compatibility*, vol. 52, no. 1, pp. 155–163, 2010.

[14] S. A. Pignari, G. Spadacini, and F. Grassi, "Modeling field-to-wire coupling in random bundles of wires," *IEEE Electromagnetic Compatibility Magazine*, vol. 6, no. 3, pp. 85–90, 2017.

[15] H. Xie, J. F. Dawson, J. Yan, A. C. Marvin, and M. P. Robinson, "Numerical and analytical analysis of stochastic electromagnetic fields coupling to a printed circuit board trace," *IEEE Transactions on Electromagnetic Compatibility*, vol. 62, no. 4, pp. 1128–1135, 2020.

[16] H. You, M. Yang, D. Wang, and X. Jia, "Kriging model combined with Latin hypercube sampling for surrogate modeling of analog integrated circuit performance," in *Proc. 10th International Symposium on Quality Electronic Design (ISQED)*, San Jose, CA, USA, pp. 554–558, 2009.

[17] J. Bai, G. Zhang, D. Wang, A. P. Duffy, and L. Wang, "Performance comparison of the SGM and the SCM in EMC simulation," *IEEE Transactions on Electromagnetic Compatibility*, vol. 58, no. 6, pp. 1739–1746, 2016.

[18] J. Bai, Y. Wan, M. Li, G. Zhang, and X. He, "Reduction of random variables in EMC uncertainty simulation model," *Applied Computational Electromagnetics Society (ACES) Journal*, vol. 37, no. 9, pp. 941–947, 2022.

[19] J. Bai, L. Wang, D. Wang, A. P. Duffy, and G. Zhang, "Validity evaluation of the uncertain EMC

simulation results," *IEEE Transactions on Electromagnetic Compatibility*, vol. 59, no. 3, pp. 797–804, 2017.

[20] C. Zhang, H. Dong, J. Ge, and H. Liu, "Theoretical channel model and characteristics analysis of EM-MWD in the underground coal mine," *IEEE Access*, vol. 9, pp. 142644–142652, 2021.



Dongxiao Pang received his Ph.D. in Mechanical Engineering from Southwest Petroleum University, China, in 2007. He currently works as a senior engineer at Chuanqing Drilling Engineering Co. Ltd. He has long been engaged in research on downhole electromagnetic wireless transmission and measurement-while-drilling (MWD) technologies, and has received multiple Science and Technology Advancement Awards from CNPC.



Huiyan Hou received the B.Eng. degree in marine electrical and electronic engineering from Dalian Maritime University, China, in 2024. She is currently a graduate student in electrical engineering at Dalian Maritime University, where her research interests include electromagnetic wave propagation and uncertainty analysis methods.



Jinjun Bai received the B.Eng. degree in electrical engineering and automation in 2013 and Ph.D. degree in electrical engineering in 2019 from the Harbin Institute of Technology, Harbin, China. He is now a lecturer at Dalian Maritime University. His research interests include uncertainty analysis methods in EMC simulation, multi-physics field simulation methods.



Xiong Han, born in October 1985, is a senior engineer and deputy director of the Technology Research and Development Centre at the Drilling and Production Institute of China Petroleum Chuanqing Drilling Engineering Co. Ltd. He was selected for the second batch of the "Youth Science and Technology Talent Training Programme" by China National Petroleum Corporation. He mainly engages in research on oil and gas wellbore communication technology, has undertaken and participated in 20 national and provincial-level research projects, holds 21 authorized invention patents, has formulated one standard, published 25 papers, and authored two monographs.